Nonuniform light-matter interaction theory for near-field-induced electron dynamics

Takeshi Iwasa
Department of Theoretical and Computational Molecular Science, Institute for Molecular Science, Myodaiji, Okazaki 444-8585, Japan

Katsuyuki Nobusada*
Department of Theoretical and Computational Molecular Science, Institute for Molecular Science, Myodaiji, Okazaki 444-8585, Japan and Department of Structural Molecular Science, School of Physical Sciences, The Graduate University for Advanced Studies, Myodaiji, Okazaki 444-8585, Japan

(Received 15 May 2009; published 13 October 2009)

A generalized theoretical description of a light-matter interaction beyond a dipole approximation is developed on the basis of the multipolar Hamiltonian with the aim of understanding the near-field excitation of molecules at the 1 nm scale. The theory is formulated for a system consisting of a molecule and a near field, where a nonuniform electric field plays a crucial role. The nonuniform light-matter interaction is expressed in terms of a spatial integral of the inner product of the total polarization of a molecule and an electric field so that the polarization is treated rigorously without invoking the conventional dipole approximation. A nonuniform electronic excitation of a molecule is demonstrated by solving a time-dependent Kohn-Sham equation in real space and real time with an implementation of the nonuniform light-matter interaction. The computations are performed to a linear chain molecule of dicyanodiacetylene (NC_6N). The nonuniform electronic excitation clearly shows inhomogeneous electron dynamics in sharp contrast to the dynamics induced by a uniform electronic excitation under the dipole approximation. Despite the inversion symmetry of NC_6N, the nonuniform excitation generates even harmonics in addition to the odd ones. Higher-order nonlinear optical response and quadrupole excitation are also observed.

DOI: 10.1103/PhysRevA.80.043409 PACS number(s): 33.80.−b, 31.15.ee, 42.65.Ky, 68.37.Uv

I. INTRODUCTION

Optical response of molecules is undoubtedly essential for understanding their physicochemical properties. For example, uv-visible light is used to study electronic states of molecules, far-infrared light for molecular vibrations, microwave for molecular rotations and so forth. In these optical responses, wavelengths of the lights are usually considered to be much longer than molecular sizes. Thus, a target molecule is well approximated by a point dipole and the dipole feels an almost uniform electromagnetic field. This condition underlies the conventional dipole approximation. Furthermore, light is an external field to excite molecules and its wavelength is definitely determined by an apparatus condition. Since spatial resolution of spectroscopy is limited by the wavelength of the incident light, it is impossible to gain molecular properties in a local region shorter than the wavelength, i.e., diffraction limit. The conventional optical response mentioned above is referred here to as a far-field and matter interaction.

However, recent development of nanofabrication and nano-optical techniques requires a more general optical response theory for the following reasons. (We note that the light is considered here to be a classical wave determined by the Maxwell equations, although it should be treated in a narrow sense by resorting to a quantum electrodynamics theory.) When noninteracting or weakly interacting nanoparticles are irradiated by an incident laser pulse, electric dipoles are induced in the nanoparticles. The induced dipoles generate local electric fields, in addition to far fields, around the nanoparticles and then the adjacent particles can interact with each other through the local fields. This local field is often referred to as a near field in contrast to a far field. The near-field interaction is significantly different from the far-field interaction [1–5]. First, as mentioned above, the near field is a local field around a particle in the presence of laser radiation and thus it is not an external field supplied from an apparatus. If the near-field irradiates adjacent particles, the new near-field is subsequently generated around the particles. The new near-field recursively irradiates other particles and these sequential light-matter interactions between the particles persist self-consistently. As a result of the self-consistent interaction, an enhanced electric field, which is closely related to surface enhanced Raman scattering (SERS) [6], appears around the particles. Such locally enhanced electric fields have been observed experimentally [7] and intensively simulated in an effort to understand mechanisms of SERS by solving the Maxwell equations [8,9]. Second, the near field is a nonpropagating wave rapidly decaying from the surface of a radiating-source particle, that is, the spatial variation of the near field is of the same order of magnitude as the particle size. Thus, the near-field interaction occurs in a narrow region comparable with the size of the particle. In other words, the near-field and matter interaction, in sharp contrast to the far-field interaction, is a nonuniform one and the spatial structure of the near field plays a crucial role. This means that the near field overcomes the diffraction limit and gives in principle information about molecular properties associated with local structures even of a 1-nm-sized nanoparticle or molecules. Conversely, those great advantages of the near-field interaction, that is, the self-consistency and the nonuniformity, require to describe light-matter interactions in a more general way.

*nobusada@ims.ac.jp; http://raphael.ims.ac.jp/

Basic frameworks of optical response taking account of the full nonuniform and self-consistent light-matter interactions have so far been developed [10–13]. Although the studies were made in various molecular or nanostructure systems at different levels of theory, the authors drew essentially the same conclusion that those full light-matter interactions have a great influence on optical properties of the systems. Very recently, to confirm the importance of the full light-matter interactions in optical response, explicit computational demonstrations have been carried out in more specific nanosystems such as nanocrystals, semiconductor quantum dots, nanoparticles, and molecular compounds [8,9,14–19]. Every study clearly showed significant effects of the full light-matter interactions beyond the dipole approximation. An electric field enhancement due to the self-consistent light-matter interaction is a key ingredient in understanding a mechanism of SERS and its computations have been intensively demonstrated as mentioned above [8,9]. Multipole effects concerning the nonuniform light-matter interaction were discussed in nanoparticles [15,16], and molecular compounds [14]. Furthermore, the self-consistent and nonuniform light-matter interactions were verified in detail to play a crucial role in optical response to localized light fields generated between nanostructures [16–18]. These explicit demonstrations have usually been done for model systems, simplifying the electronic structures of target nanostructures, for example, the nanostructures were assumed to be dielectric particles or their optical susceptibilities were given in advance. This is partly because it is computationally highly demanding to fully quantum-mechanically solve electron dynamics of the target nanosystems coupled with the electromagnetic field dynamics, in particular almost impossible for real nanostructures in a 1 nm size or more. Nevertheless, in molecular science, it is essential to calculate optical properties associated with details of electronic structures, such as geometric structures, bond characters, charge distribution, and electron correlation, of target nanostructures. To describe optical response of 1-nm-sized molecules, we split the full-light matter interaction into the issues of self-consistency and nonuniformity. We first consider the nonuniform light-matter interaction as an initial step and leave the self-consistent interaction (i.e., solving the Maxwell-Schrödinger coupled equation) for the next. Here, a first-principles approach to treat a nonuniform light-matter interaction in real molecular systems is developed. We place special emphasis on obtaining full quantum-mechanical solutions of electron dynamics under the near field (i.e., local field) to elucidate the nonuniform light-mater interaction at the level of molecular theory.

The conventional optical response theory is usually formulated starting from the minimal coupling Hamiltonian, and the formulation often relies on the dipole approximation. In contrast, we develop a more general theory without the dipole approximation, on the basis of the multipolar Hamiltonian derived from the minimal coupling Hamiltonian by a canonical transformation [11,20–22]. The light-matter interaction in the multipolar Hamiltonian is described in terms of the space integral of an inner product of polarization and an electric field, whereas the minimal coupling Hamiltonian uses momentum and vector potential. The last two variables are rather inconvenient for practical calculations. Noteworthy is the fact that in the multipolar Hamiltonian approach the polarization in the integral can be treated entirely without any approximations. This means that infinite orders of multipole moments are taken into account. Therefore, the present approach is a generalization of the conventional optical response theory with the dipole approximation.

To investigate optical properties of real molecules, explicit time evolution of electron dynamics should be solved. To this end, we have incorporated our optical response theory with the nonuniform light-matter interaction into our developed electron-dynamics simulation approach in real space [23–26] based on time-dependent density functional theory (TDDFT). The integrated TDDFT approach has been applied to and computationally solved for a test molecular system of dicyanodiacetylene (NC_6N) as an example, to elucidate the electron dynamics of 1-nm-sized molecules induced by the nonuniform near field.

The structure of this paper is as follows. Section II develops an optical response theory of the nonuniform light-matter interaction on the basis of the multipolar Hamiltonian. The nonuniform light-matter interaction formula is further implemented into the TDDFT simulation approach with the aim of elucidating the near-field excitation mechanisms of 1-nm-sized molecules. Section III explains a theoretical model of the near-field interaction and methods of computations. In Sec. IV, computed results and their analysis are presented. The concluding remarks are made in Sec. IV. The SI unit is used and all the operators are hatted throughout this paper.

II. THEORY

A. Multipolar Hamiltonian

As mentioned in the previous section, we start our theoretical formulation from the multipolar Hamiltonian to include full spatial variation of an electric field for the nonuniform light-matter interaction. It should be noted that in this study the electric field is considered to be a classical value and any magnetic interactions are neglected. The intermolecular distances are assumed to be large enough so that their electronic wave functions do not overlap. The multipolar Hamiltonian of nonoverlapping molecules interacting with an electric field is then obtained as [22]

$$\hat{H} = \hat{H}_{\mathrm{mol}} + \hat{V}_{\mathrm{inter}} - \int d\boldsymbol{r}\hat{\boldsymbol{P}}(\boldsymbol{r}) \cdot \boldsymbol{E}^{\perp}(\boldsymbol{r},t), \tag{1}$$

where $\hat{H}_{\mathrm{mol}}$ is the Hamiltonian of the molecules and $\hat{V}_{\mathrm{inter}}$ is the static intermolecular Coulomb interaction. $\hat{\boldsymbol{P}}(\boldsymbol{r}) = \Sigma_i \hat{\boldsymbol{P}}_i(\boldsymbol{r})$ is the total polarization operator of the system with $\hat{\boldsymbol{P}}_i(\boldsymbol{r})$ being the polarization operator of the molecule i. $\boldsymbol{E}^{\perp}(\boldsymbol{r},t)$ is the transverse part of the electric field written in the form of

$$\boldsymbol{E}^{\perp}(\boldsymbol{r},t) = \boldsymbol{E}^{\perp}_{\mathrm{laser}}(\boldsymbol{r},t) + \sum_j \boldsymbol{E}^{\perp}_j(\boldsymbol{r},t), \tag{2}$$

where $\boldsymbol{E}^{\perp}_{\mathrm{laser}}(\boldsymbol{r},t)$ is an incident laser field and $\boldsymbol{E}^{\perp}_j(\boldsymbol{r},t)$ is the electric field radiated from the jth molecule obtained by solving the Maxwell equations using $\boldsymbol{P}^{\perp}_j(\boldsymbol{r}', t-|\boldsymbol{r}-\boldsymbol{r}'|/c)$ as a

source with c being the speed of light. The static intermolecular Coulomb interaction is given by

$$\hat{V}_{\text{inter}} = \frac{1}{\varepsilon_0}\sum_{i<j}\int d\boldsymbol{r}\hat{\boldsymbol{P}}_i^{\parallel}(\boldsymbol{r})\cdot\hat{\boldsymbol{P}}_j^{\parallel}(\boldsymbol{r}), \tag{3}$$

where $\hat{\boldsymbol{P}}_i^{\parallel}(\boldsymbol{r})$ is the longitudinal part of $\hat{\boldsymbol{P}}_i(\boldsymbol{r})$. Then, Eq. (1) is rewritten as

$$\hat{H} = \hat{H}_{\text{mol}} + \frac{1}{\varepsilon_0}\sum_{i<j}\int d\boldsymbol{r}\hat{\boldsymbol{P}}_i^{\parallel}(\boldsymbol{r})\cdot\hat{\boldsymbol{P}}_j^{\parallel}(\boldsymbol{r}) - \sum_i\int d\boldsymbol{r}\hat{\boldsymbol{P}}_i(\boldsymbol{r})\cdot\boldsymbol{E}^{\perp}(\boldsymbol{r},t). \tag{4}$$

The explicit form of $\hat{\boldsymbol{P}}_i(\boldsymbol{r})$ is [20–22]

$$\hat{\boldsymbol{P}}_i(\boldsymbol{r}) = \sum_{\alpha} e_{\alpha}(\hat{\boldsymbol{q}}_{\alpha}-\boldsymbol{R}_i)\int_0^1 d\lambda\,\delta[\boldsymbol{r}-\boldsymbol{R}_i-\lambda(\hat{\boldsymbol{q}}_{\alpha}-\boldsymbol{R}_i)], \tag{5}$$

where e_{α} and $\hat{\boldsymbol{q}}_{\alpha}$ are the charge and the position operator of the αth electron in the molecule i, respectively, and $\boldsymbol{R}_i$ is the center of mass of the molecule. The integration in Eq. (5) with respect to λ is introduced to express the polarization in such a compact form, instead of using multipoles explicitly.

We address here the relation between our optical response formula and the conventional approach based on a multipole expansion method. Equation (5) can be expanded in a Taylor series leading to the dipole, quadrupole, octapole, and higher-order multipole terms. The present formulation is thus a generalization of the conventional optical response theory with the dipole approximation. Applying the Taylor expansion to Eq. (5) and integrating the resulting equation with respect to λ, we obtain

$$\begin{aligned}
&\int d\boldsymbol{r}\hat{\boldsymbol{P}}(\boldsymbol{r})\cdot\boldsymbol{E}^{\perp}(\boldsymbol{r},t)\\
&= \left[\sum_{\alpha} e_{\alpha}(\hat{\boldsymbol{q}}_{\alpha}-\boldsymbol{R})_i\right]\cdot E_i^{\perp}(\boldsymbol{R},t)\\
&\quad - \left[\frac{1}{2!}\sum_{\alpha} e_{\alpha}(\hat{\boldsymbol{q}}_{\alpha}-\boldsymbol{R})_i(\hat{\boldsymbol{q}}_{\alpha}-\boldsymbol{R})_j\right]\nabla_i E_j^{\perp}(\boldsymbol{R},t)\\
&\quad + \left[\frac{1}{3!}\sum_{\alpha} e_{\alpha}(\hat{\boldsymbol{q}}_{\alpha}-\boldsymbol{R})_i(\hat{\boldsymbol{q}}_{\alpha}-\boldsymbol{R})_j(\hat{\boldsymbol{q}}_{\alpha}-\boldsymbol{R})_k\right]\\
&\quad \times \nabla_i\nabla_j E_k^{\perp}(\boldsymbol{R},t) - \cdots\\
&\equiv \hat{\mu}_i E_i^{\perp} + \hat{Q}_{ij}\nabla_i E_j^{\perp} + \hat{O}_{ijk}\nabla_i\nabla_j E_k^{\perp} + \cdots,
\end{aligned} \tag{6}$$

where $\hat{\mu}_i$, $\hat{Q}_{ij}$, and $\hat{O}_{ijk}$ represent the dipole, quadrupole, and octapole moments of a molecule, respectively, and the indexes denote their (x,y,z) tensorial components. These moments are defined at the molecular center $\boldsymbol{R}$. ∇_i is the gradient operator along the ith direction and acts on the electric field. We here use a contraction of $x_i y_i = \Sigma_i x_i y_i$. The dipole moment couples with the field itself, the quadrupole with the first derivative of the field, and the octapole with the second derivative of the field, and so forth. If an electric field varies slowly over a whole spatial region, the optical response can be reasonably described by only the first term of this expansion (i.e., the dipole approximation). However, the near-field interaction requires an infinite number of terms in the expansion because of its nonuniform spatial structure. Therefore, we use Eq. (5) as is, without performing the Taylor expansion of the polarization.

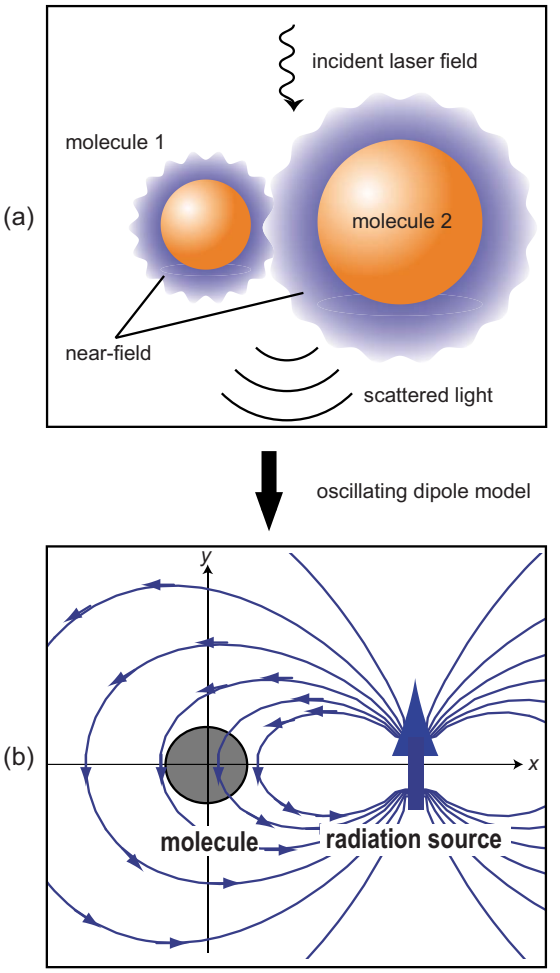

FIG. 1. (Color online) (a) Schematic of near-field and scattered light radiation from distant molecules 1 and 2 in the presence of an incident laser field. (b) Nonuniform light-matter interaction model derived from the above molecular system. The molecule 2 is considered to be a radiation source approximated by an oscillating dipole (a blue bold arrow). The near fields, i.e., nonuniform electric fields, radiated from the oscillating dipole are shown in the blue curves.

B. Molecule interacting with a near-field

To demonstrate the electron dynamics in molecules interacting with a near field, we first introduce a theoretical model consisting of two molecules irradiated by a laser light. Figure 1(a) schematically shows the model. The multipolar Hamiltonian Eq. (4) is rewritten for such a model system by

$$\hat{H}_{\text{mol}} + \frac{1}{\varepsilon_0}\int d\boldsymbol{r}\hat{\boldsymbol{P}}_1^{\parallel}(\boldsymbol{r})\cdot\hat{\boldsymbol{P}}_2^{\parallel}(\boldsymbol{r}) - \int d\boldsymbol{r}[\hat{\boldsymbol{P}}_1(\boldsymbol{r})+\hat{\boldsymbol{P}}_2(\boldsymbol{r})]\cdot\boldsymbol{E}^{\perp}(\boldsymbol{r},t). \tag{7}$$

As mentioned in the beginning of this paper, the near field is a nonpropagating local field around nanostructures, gener-

ated in the presence of laser irradiation. Although the near field should be given by solving the Maxwell equations (or by resorting to quantum electrodynamics theory in a narrow sense), it is reasonably approximated by the short-range term of an oscillating dipole radiation [4,27]. Then, the theoretical model given by Eq. (7) can be further simplified as follows. We discuss here optical response of the molecule 1 interacting only with the near field radiated from the molecule 2, in which the molecule 2 is considered to be an oscillating dipole as shown in Fig. 1(b). This approximation means that the material Hamiltonian of the molecule 1 is solved quantum mechanically, whereas the molecule 2 is assumed to be a classical dielectric merely as a radiation source. Furthermore, we neglect the near field induced around the molecule 1, which might affect the dielectric molecule 2 (i.e., the self-consistent effect) when the molecule 1 is electronically excited in its resonance state [16,18]. Since we focus on roles of the nonuniform electric field in electronic excitation of a molecule, the near-field frequency is chosen so that the resonance excitation does not occur principally. In addition, if the molecule 1 is smaller than the molecule 2, its induced polarization is also relatively smaller than that of the molecule 2. Thus, it is reasonable for the moment to neglect the induced near field around the molecule 1. In other words, our light-matter interaction model is expected to be useful for studies about spatially resolved local spectroscopy taking advantage of the nonuniform light-matter interaction in real molecules because radiations from target molecules are usually weak compared to those of probe tips. For these reasons, the self-consistent effect is left for the future investigation. The incident laser field $\boldsymbol{E}_{\mathrm{laser}}^{\perp}$ in the third term of Eq. (7) is required to induce the polarization associated with the oscillating dipole in the molecule 2. From our preliminary calculations, however, the incident field was found to be less important for the light-matter interaction in the near-field region because the intensity of the induced near field is larger than that of the incident field. As a result, the electron dynamics in this region is qualitatively unaffected even if the incident laser field is neglected.

Under these conditions, Eq. (7) can be reduced to the form of

$$\hat{H}_{\mathrm{mol}} - \int d\boldsymbol{r}\hat{\boldsymbol{P}}_1^{\parallel}(\boldsymbol{r}) \cdot \tilde{\boldsymbol{E}}_2^{\parallel}(\boldsymbol{r},t) - \int d\boldsymbol{r}[\hat{\boldsymbol{P}}_1(\boldsymbol{r}) + \hat{\boldsymbol{P}}_2(\boldsymbol{r})] \cdot [\tilde{\boldsymbol{E}}_1^{\perp}(\boldsymbol{r},t) + \tilde{\boldsymbol{E}}_2^{\perp}(\boldsymbol{r},t)], \quad (8)$$

where the longitudinal part of the polarization operator $\hat{\boldsymbol{P}}_2^{\parallel}$ is replaced with the expectation (or c-number) value $-\varepsilon_0\tilde{\boldsymbol{E}}_2^{\parallel}$ in the vicinity of the molecule 1. $\tilde{\boldsymbol{E}}$ represents the near-field part of $\boldsymbol{E}$. Although the far-field part of $\boldsymbol{E}$ can also be included in this derivation, we only use the near-field part for simplicity. Equation (8) is rewritten in a more compact form of

$$\hat{H}_{\mathrm{mol}} - \int d\boldsymbol{r}\hat{\boldsymbol{P}}_1(\boldsymbol{r}) \cdot \tilde{\boldsymbol{E}}_2(\boldsymbol{r},t) - \int d\boldsymbol{r}\{\hat{\boldsymbol{P}}_1(\boldsymbol{r}) \cdot \tilde{\boldsymbol{E}}_1^{\perp}(\boldsymbol{r},t) + \hat{\boldsymbol{P}}_2(\boldsymbol{r}) \cdot [\tilde{\boldsymbol{E}}_1^{\perp}(\boldsymbol{r},t) + \tilde{\boldsymbol{E}}_2^{\perp}(\boldsymbol{r},t)]\}, \quad (9)$$

where we used the relations of $\hat{\boldsymbol{P}}_1^{\parallel} \cdot \tilde{\boldsymbol{E}}_2^{\parallel} = \hat{\boldsymbol{P}}_1 \cdot \tilde{\boldsymbol{E}}_2^{\parallel}$ and $\tilde{\boldsymbol{E}}_2^{\parallel} + \tilde{\boldsymbol{E}}_2^{\perp} = \tilde{\boldsymbol{E}}_2$. Since the self-interaction term $\hat{\boldsymbol{P}}_1 \cdot \tilde{\boldsymbol{E}}_1^{\perp}$ is not important in this work and $\hat{\boldsymbol{P}}_2 \cdot (\tilde{\boldsymbol{E}}_1^{\perp} + \tilde{\boldsymbol{E}}_2^{\perp})$ does not act on the molecule 1, these terms can be omitted. Finally, the Hamiltonian of a molecule interacting with the near-field becomes

$$\hat{H} \equiv \hat{H}_{\mathrm{mol}} + \hat{H}_{\mathrm{int}}(t) = \hat{H}_{\mathrm{mol}} - \int d\boldsymbol{r}\hat{\boldsymbol{P}}_1(\boldsymbol{r}) \cdot \tilde{\boldsymbol{E}}_2(\boldsymbol{r},t), \quad (10)$$

This nonuniform light-matter interaction Hamiltonian is used throughout this study. Our computational model is rather oversimplified. However, it is computationally demanding (might be practically impossible) to fully solved coupled Schrödinger-Maxwell equations, taking account of the properties of the self-consistency and the nonuniformity due to the light-matter interaction at the 1 nm scale. This derivation can also be applied to three or more particle systems, where only the dynamics of the molecule 1 interacting with the near-fields generated by the molecules 2,3,... is solved quantum mechanically in a similar way as in the two-particle system.

C. Near-field radiated from an oscillating dipole

We have next to model the near field. The near field is known to be a localized, nonpropagating part of the light generated from a molecule when irradiated by an incident laser field [see Fig. 1(a)]. We describe the near field in this paper as the near part of the electric field generated from an oscillating dipole, the simplest model for a radiation. In Fig. 1(b), the electric lines of the dipole radiation are depicted as the blue curves, the directions of which are shown by the arrows on the lines.

The analytical expression of the dipole radiation field $\boldsymbol{E}_{\mathrm{dip}}(\boldsymbol{r},t)$ generated by the oscillating dipole is given by [27]

$$\boldsymbol{E}_{\mathrm{dip}}(\boldsymbol{r},t) = \frac{k^3}{4\pi\varepsilon_0}\left(\frac{[3\boldsymbol{n}(\boldsymbol{n}\cdot\boldsymbol{\mu}) - \boldsymbol{\mu}]}{(kr)^3}\right. \quad (11a)$$

$$- i\frac{[3\boldsymbol{n}(\boldsymbol{n}\cdot\boldsymbol{\mu}) - \boldsymbol{\mu}]}{(kr)^2} \quad (11b)$$

$$\left. + \frac{[(\boldsymbol{n}\times\boldsymbol{\mu})\times\boldsymbol{n}]}{(kr)}\right)e^{-i\omega t + ikr} \quad (11c)$$

where k is a wave number, ε_0 is the vacuum permittivity, $\boldsymbol{n}$ is the unit vector of $\boldsymbol{r}/r$, $\boldsymbol{\mu}$ is a dipole moment of the source placed at the origin, and ω is a frequency of the oscillation, where $\omega = kc$ with c being the velocity of light. The radiation field is classified into three parts in terms of the radial dependencies, r^{-3}, r^{-2}, and r^{-1}. We set the distance between the target molecule and the radiation source to be several angstroms, which is comparable in size with the molecule. In this region, the dipole radiation field is dominated by the local electric field depending on r^{-3} given by Eq. (11a). This local field is referred to as the near-field $\tilde{\boldsymbol{E}}$ used in the nonuniform light-matter interaction in Eq. (10). We can then neglect the magnetic interacting terms because the magnetic field from the oscillating dipole, not shown here, has the r^{-2} and r^{-1} dependent terms.

Since we consider an optical interaction between very closely spaced particles, it is reasonable to use the dipole radiation field as the electric near-field $\tilde{\boldsymbol{E}}_2$ without distinguishing its longitudinal and transverse components. For larger systems, however, the longitudinal and transverse parts should be evaluated separately because there is a difference in time between them, i.e., the longitudinal interaction is instantaneous, whereas the transverse one is retarded. The retardation effect can be treated by solving the Maxwell equations using the time-dependent polarization as a radiation source.

D. Light-matter interaction in the Kohn-Sham equation

For computational applications of the present formal theory, we will derive the light-matter interaction H_{int} in the Kohn-Sham (KS) DFT form. In the following derivations, we take $e_\alpha=-1$ for simplicity. Although the KS Hamiltonian is obtained by functional derivative of the expectation value of the total energy, it is enough to consider here only the light-matter interaction term of Eq. (10). The expectation value of $\hat{H}_{\text{int}}$ is expressed by

$$\begin{aligned}
\langle \hat{H}_{\text{int}}(t)\rangle &= \int d\boldsymbol{r}\Psi^*(\boldsymbol{r},t)\hat{H}_{\text{int}}(t)\Psi(\boldsymbol{r},t) \\
&= -\int d\boldsymbol{r}d\boldsymbol{r}'\Psi^*(\boldsymbol{r},t)\hat{\boldsymbol{P}}(\boldsymbol{r}')\Psi(\boldsymbol{r},t)\cdot\tilde{\boldsymbol{E}}(\boldsymbol{r}',t) \\
&= \int d\boldsymbol{r}d\boldsymbol{r}'\Psi^*(\boldsymbol{r},t)(\boldsymbol{r}-\boldsymbol{R}) \\
&\quad\times\int_0^1 d\lambda\,\delta[\boldsymbol{r}'-\boldsymbol{R}-\lambda(\boldsymbol{r}-\boldsymbol{R})]\Psi(\boldsymbol{r},t)\cdot\tilde{\boldsymbol{E}}(\boldsymbol{r}',t) \\
&= \int d\boldsymbol{r}[\Psi^*(\boldsymbol{r},t)\Psi(\boldsymbol{r},t)](\boldsymbol{r}-\boldsymbol{R})\int_0^1 d\lambda \\
&\quad\times\int d\boldsymbol{r}'\,\delta[\boldsymbol{r}'-\boldsymbol{R}-\lambda(\boldsymbol{r}-\boldsymbol{R})]\tilde{\boldsymbol{E}}(\boldsymbol{r}',t) \\
&\equiv \int d\boldsymbol{r}\rho(\boldsymbol{r},t)(\boldsymbol{r}-\boldsymbol{R})\cdot\int_0^1 d\lambda\tilde{\boldsymbol{E}}[\boldsymbol{R}+\lambda(\boldsymbol{r}-\boldsymbol{R}),t] \\
&\equiv \int d\boldsymbol{r}\rho(\boldsymbol{r},t)(\boldsymbol{r}-\boldsymbol{R})\cdot\boldsymbol{E}_{\text{eff}}(\boldsymbol{r},t) \\
&\equiv \int d\boldsymbol{r}\rho(\boldsymbol{r},t)V_{\text{eff}}(\boldsymbol{r},t) \qquad (12)
\end{aligned}$$

where Ψ is the ground-state wave function of the molecule, and the electron density $\rho(\boldsymbol{r})$, the effective electric field $\boldsymbol{E}_{\text{eff}}$, and the effective potential V_{eff} are given by

$$\rho(\boldsymbol{r},t)\equiv\Psi^*(\boldsymbol{r},t)\Psi(\boldsymbol{r},t), \qquad (13)$$

$$\boldsymbol{E}_{\text{eff}}(\boldsymbol{r},t)\equiv\int_0^1 d\lambda\tilde{\boldsymbol{E}}[\boldsymbol{R}+\lambda(\boldsymbol{r}-\boldsymbol{R}),t], \qquad (14)$$

$$V_{\text{eff}}(\boldsymbol{r},t)\equiv(\boldsymbol{r}-\boldsymbol{R})\cdot\boldsymbol{E}_{\text{eff}}(\boldsymbol{r},t). \qquad (15)$$

The λ-integration of $\tilde{\boldsymbol{E}}$ includes all the contributions of the spatial variation of the electric field. As is clearly seen from Eq. (12), the nonuniform light-matter interaction is straightforwardly calculated in the conventional KS-DFT approach if the effective potential V_{eff} is added to the external potential term in the KS equation. In the next section, the KS-DFT computational approach will be explained to demonstrate the electron dynamics of nanoclusters interacting with a near-field.

III. COMPUTATIONAL APPLICATION

A. Time-dependent Kohn-Sham approach in real space

The time-dependent Kohn-Sham (TD-KS) approach in real space and time to electron dynamics has so far been explained elsewhere [23,28–30]. We review the approach with particular emphasis on extending it to the optical response to a nonuniform electric field. A time-dependent N-electron interacting system is solved through a set of electronic wave functions $\psi_j(\mathbf{r},t)$ satisfying the following TD-KS equation

$$i\hbar\frac{\partial}{\partial t}\psi_j(\mathbf{r},t)=\left[-\frac{\hbar^2}{2m}\nabla^2+V_{\text{KS}}[\rho](\mathbf{r},t)\right]\psi_j(\mathbf{r},t), \qquad (16)$$

where m is the electron mass and ρ is the electron density given by

$$\rho(\mathbf{r},t)=2\sum_{j=1}^{N/2}|\psi_j(\mathbf{r},t)|^2. \qquad (17)$$

The factor of 2 indicates that each KS orbital is fully occupied (i.e., a closed shell system). The KS potential $V_{\text{KS}}[\rho](\mathbf{r},t)$ is a functional of ρ, and it consists of four terms of an ion-electron interaction potential $V_{\text{ion}}(\mathbf{r})$, a time-dependent Hartree potential, an exchange-correlation (xc) potential $V_{\text{xc}}[\rho](\mathbf{r},t)$, and an external potential V_{eff} as follows:

$$\begin{aligned}
V_{\text{KS}}[\rho](\mathbf{r},t) &= V_{\text{ion}}(\mathbf{r})+\frac{1}{4\pi\varepsilon_0}\int\frac{\rho(\mathbf{r}',t)}{|\mathbf{r}-\mathbf{r}'|}d\mathbf{r}'+V_{\text{xc}}[\rho](\mathbf{r},t) \\
&\quad+V_{\text{eff}}(\mathbf{r},t). \qquad (18)
\end{aligned}$$

The ion-electron interaction potential $V_{\text{ion}}(\mathbf{r})$ is constructed from norm-conserving pseudopotentials of each atomic component of the system considered. Following the Troullier and Martins procedure [31], the pseudopotentials are numerically generated so that the pseudowave functions can imitate the all-electron atomic wave functions. The potentials depend on the angular momentum components. In this paper, we use the Kleinman-Bylander separable form to represent the nonlocal (i.e., angular momentum depending) potential terms [32].

To represent the xc potential, we use the following adiabatic local density approximation (ALDA)

$$V_{\mathrm{xc}}[\rho](\mathbf{r},t) \approx V_{\mathrm{xc}}^{\mathrm{LDA}}[\rho](\mathbf{r},t) = V_{\mathrm{xc}}^{\mathrm{LDA}}[\rho_0](\mathbf{r})|_{\rho_0(\mathbf{r})=\rho(\mathbf{r},t)}, \tag{19}$$

where $V_{\mathrm{xc}}^{\mathrm{LDA}}[\rho_0](\mathbf{r})$ is the ground-state LDA xc potential given by Perdew and Zunger [33]. In ALDA, the xc potential at $\mathbf{r}$ and t is approximated by that of the ground-state uniform electron gas having the density $\rho(\mathbf{r},\mathbf{t})$. Although the ALDA xc potential does not take account of the nonlocality in both $\mathbf{r}$ and t and more accurate exchange-correlation functionals have been developed lately, the ALDA has practically provided reasonable results for single-electron excitation processes sufficiently below the lowest ionization threshold of systems [34–36]. Furthermore, it is reasonable to use such a simple functional at this early stage of development prior to performing highly accurate calculations toward material science.

In the present theoretical model of the nonuniform light-matter interaction, the external potential V_{eff} is given by Eqs. (14) and (15). As mentioned above, $\tilde{\boldsymbol{E}}$ in Eq. (14) is approximated as the oscillating dipole radiation Eq. (11), the main contribution of which is given by the r^{-3} dependent term of Eq. (11a). We set the center of mass of the molecule to be the origin. The temporal shape of the near field is taken as a pulse. Finally, the effective potential Eq. (15) is rewritten by

$$V_{\mathrm{eff}}(\mathbf{r},t) = -\boldsymbol{r}\cdot\boldsymbol{E}_{\mathrm{eff}}(\boldsymbol{r})\sin(\omega t)\sin^2\left(\frac{\pi t}{T}\right)(0<t<T), \tag{20}$$

where ω is the frequency of the oscillating dipole, and T determines the pulse duration. The pulse profile is approximated by $\sin^2(\frac{\pi t}{T})$ in which a few cycles of the electric fields are included. The field intensity is related to the field strength by $I=\frac{1}{2}\varepsilon_0 cE^2$.

B. Molecular system and computational details

A linear chain molecule is one of the better choices to demonstrate the nonuniform light-matter interaction, in particular for such an electric field proportional to r^{-3}. We choose a dicyanodiacetylene (NC_6N) molecule [37] shown in Fig. 2(a) as an example of a real molecule. The geometric structure has been optimized by using the TURBOMOLE V5.10 [38,39] package of quantum chemistry programs, employing the LDA exchange functional developed by Perdew and Wang [40] with the basis set of def-SV(P) [41] from the TURBOMOLE basis set library, which corresponds to the basis set of 6-31G*. The simplest functional LDA was chosen for consistency with the functional used in the TD-KS equation. The vibrational analysis showed no imaginary frequency. The interatomic distances of the molecule are N_1-C_2 =1.176 Å, C_2-C_3=1.354 Å, C_3-C_4=1.239 Å, and C_4-C_5 =1.340 Å [42].

The TDKS Eq. (16) for NC_6N is solved numerically by a grid-based method [23,43] in a three-dimensional Cartesian-coordinate rectangular box, the lengths of which are 30 Å along the molecular (x-) axis and 20 Å along the y and z axes, utilizing uniform grids with a mesh spacing of 0.3 Å. The Laplacian operator is evaluated by a nine-point difference formula [44]. The time propagation of the KS orbitals is carried out with a fourth-order Taylor expansion by using a constant time step of 0.002 fs. The inner shell structures of the carbon and nitrogen atoms are approximated by effective core pseudopotentials, and then the remaining four electrons ($2s^22p^2$) for C and five electrons ($2s^22p^3$) for N are explicitly treated. In other words, we have carried out 34-electron dynamics calculations for NC_6N.

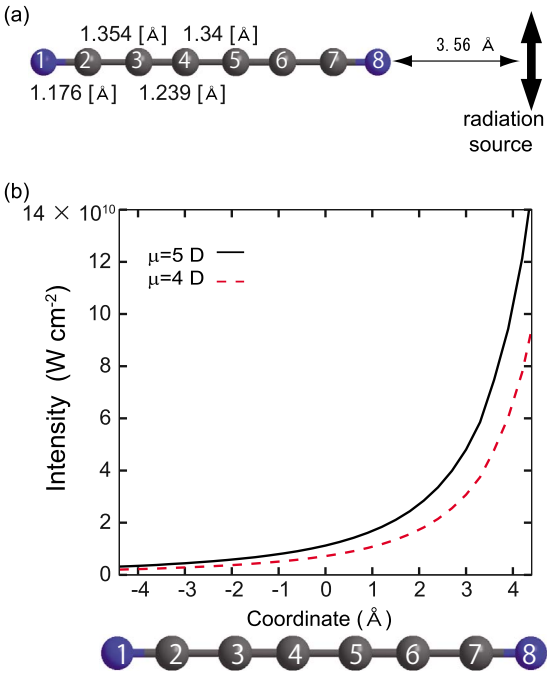

FIG. 2. (Color online) (a) Geometrical structure of NC_6N and the position of the radiation source. (b) The intensities of the effective electric fields on the molecular axis calculated from the near field of the dipole radiation. The near fields are generated by the oscillating dipole with its absolute value of the dipole moment being 4 D (dashed red line) and 5 D (black line), respectively.

The effective potential for the dipole radiation on each grid is computed combining Eqs. (11), (14), and (15), where the main contribution in Eq. (11) is its near-field part (11a). A point dipole $\boldsymbol{\mu}$ is placed at x=8.0 Å [i.e., the value of 3.56 Å is the distance between the rightmost nitrogen atom N(8) and the dipole as shown in Fig. 2(a)] so that the nonuniform electronic excitation due to the near-field is clearly demonstrated. The dipole is assumed to be y polarized, that is $\boldsymbol{\mu}=(0.0,\mu,0.0)$ debye (D), where μ is the absolute value of the dipole moment. The dipole fields generated from μ =4.0 D and 5.0 D are used in this study. The integral of Eq. (14) is calculated numerically with a constant step of $\Delta\lambda$ =0.0423 Å. The contribution of the dipole radiation field at its origin to the integration is evaluated by $4\pi\boldsymbol{\mu}/3$ [22]. $\boldsymbol{E}_{\mathrm{dip}}$ is also replaced with $4\pi\boldsymbol{\mu}/3$ if $|\boldsymbol{E}_{\mathrm{dip}}|$ is larger than $|4\pi\boldsymbol{\mu}/3|$. This is done for a few points very close to the dipole, i.e., $|r|\sim 0.2$ Å. The intensity of the effective electric field varies largely as indicated in Fig. 2(b). The effective field intensity at the right end of the NC_6N molecule is two orders of magnitude larger than that at the left end (i.e., 10^{11} and 10^9 W/cm^2 at the right and the left ends, respectively). Thus, the molecule is nonuniformly excited by the oscillating

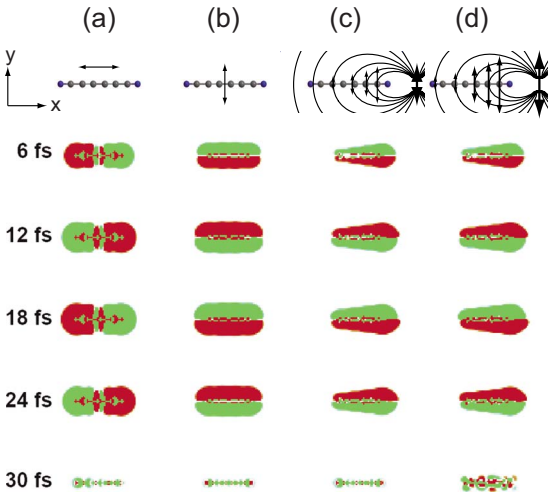

FIG. 3. (Color online) Snapshots of difference of the electron density at $t=6$, 12, 18, 24, and 30 fs from the initial ($t=0$ fs) static electron density. The uniform fields [(a), (b)] and the nonuniform (oscillating dipole) fields with their dipole moments being (c) 4 D and (d) 5 D are applied to the molecule. The red (black) and green (light gray) colors represent an increase and a decrease in the electron density, respectively. Four schematic illustrations at the top of each snapshot display the ways of electronic excitation.

dipole field. All the electric fields used in this study have the field frequency ω of 1 eV (the off-resonance condition). The pulse duration ($T=30$ fs) is short enough to avoid considering the nuclear dynamics.

IV. RESULTS AND DISCUSSION

A. Nonuniform electronic excitation

Let us first demonstrate the electron-density motions in the uniform and the nonuniform electric fields. Figure 3 shows four snapshots of differences of the electron densities at $t=6$, 12, 18, 24, and 30 fs from the initial ($t=0$) electron density. The red (black) and green (light gray) colors indicate an increase and a decrease in the electron density, respectively. Each column of the snapshots illustrates the different time evolution of the electron density depending on the ways of electronic excitation. Four schematic illustrations at the top of the figure display how the light-matter interaction works. The uniform oscillating-electric-field with its intensity of 10^{12} W/cm^2 is applied to the molecule along the (a) x or (b) y axis, whereas the nonuniform fields radiated from the oscillating dipoles (the black bold arrows) with their dipole moments being (c) 4 D and (d) 5 D are applied to the molecule.

The electron densities in Figs. 3(a) and 3(b) oscillate uniformly and regularly along the applied field directions, keeping the molecular symmetry. However, as shown in Figs. 3(c) and 3(d), the nonuniform electric field apparently induces the symmetry-breaking time evolution of the electron density. Such inhomogeneous electron dynamics clearly reflects the spatial distribution of the dipole field. Since the oscillating dipole is y polarized, the generated electric field on the x axis is also y polarized, but its intensity sharply falls as r increases (i.e., $\propto r^{-3}$), where r is the distance from the oscillating dipole. Furthermore, only the x component of the dipole field E_x is antisymmetric with respect to the x axis [i.e., $E_x(x,y,z)=-E_x(x,-y,z)$], whereas E_y and E_z are symmetric. For these reasons, the time-evolved densities in Figs. 3(c) and 3(d) regularly oscillate to some extent along the y axis, whereas those are distorted along the x axis. The electron-density distributions at 12 and 18 fs, for example, represent the antisymmetric motion along the x axis. Specifically, the upper and lower half parts of the densities with respect to the x axis move toward the opposite directions. These irregular motions are really due to the electronic excitation by the symmetry-breaking, nonuniform electric field. The electron-density distribution at 30 fs in Fig. 3(d) looks rather different from the others. The electron-density-differences in Figs. 3(a)–3(c) almost disappear at the end of the pulse of the external electric fields because the applied laser frequency considered is not in tune with any resonance frequencies. In contrast, the electron-density distribution in Fig. 3(d), under the condition of the stronger nonuniform electric field, still persists even after the end of the pulsed near field. This is attributed to the nonuniform excitation by the localized near field. In this study, the near-field frequency is not tune with any dipole resonance frequencies of NC_6N. Thus, the time evolution of the electron density should not persist after the end of the near-field radiation [see, Fig. 3(c)]. However, higher harmonics are more easily generated by the nonuniform excitation with increasing the strength of the dipole radiation field. NC_6N has a dipole resonance frequency at 5.75 eV, which is close to the sixth harmonics (=6 eV). As the result of this, the resonance excitation accidentally occurs in the case of Fig. 3(d). Such a resonance excitation allows the electrons to move persistently after the end of the pulse. It should be noted that this resonance effect is due to a high-order nonlinear effect and thus is still minor in the present nonuniform light-matter interaction model, i.e., it hardly affects the radiation from the molecule 2.

Figures 4(a)–4(d) show the induced dipole moments along the x and y axes, $d_i(i=x,y)$, corresponding to the time evolutions of the electron densities in Figs. 3(a)–3(d), respectively. The red and the dashed black curves represent d_x and d_y. The insets in Figs. 4(a) and 4(b) schematically draw the applied field directions. Similar overall time-profiles have been observed in d_x [Fig. 4(a)] and d_y [Fig. 4(b)] induced by the uniform field and in d_y induced by the nonuniform field. In sharp contrast, nonuniformly induced d_xs do not follow the time profile of the applied field. To see this more clearly, we pick up d_x in Fig. 4(d) and plot it in Fig. 5. In the early times until about 20 fs, d_x takes negative values owing to the sharp gradient in the field intensity. The oscillation frequency becomes much faster than that of the applied field after ~20 fs. Such an irregular oscillation of d_x is a consequence of the antisymmetric E_x of the dipole field that acts strongly in the right part of NC_6N. Thus, the irregular time evolutions of the density along the x axis in Figs. 3(c) and 3(d) were induced by the nonuniform, antisymmetric dipole radiation field. We have further confirmed that such an irregular motion cannot be induced even if we use either an electric field having a similar sharp gradient in the field intensity or an antisymmetric electric field.

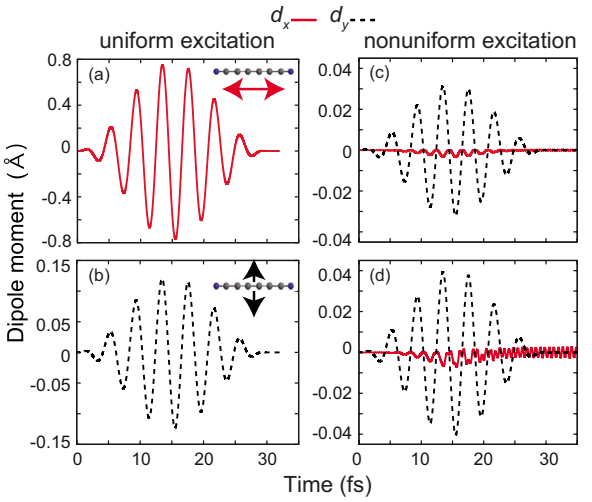

FIG. 4. (Color online) Induced dipole moments along the x and y axes, $d_i(i=x,y)$. The dipole moments, respectively, correspond to the time evolutions of the density in Figs. 3(a)–3(d). Insets in (a) and (b) are schemes of the applied field direction.

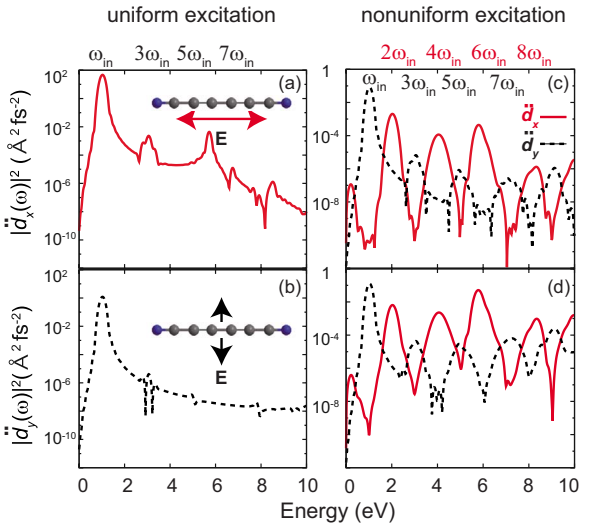

FIG. 6. (Color online) Power spectra of the dipole acceleration. The ways of electronic excitation correspond to those in Figs. 3(a)–3(d) and also in Figs. 4(a)–4(d), respectively.

We next calculate the emission spectra for each electron dynamics to analyze the uniform and nonuniform electronic excitations in an energy domain. Since the emission spectrum is associated with the dipole acceleration [45,46], we here take the second derivative of the induced dipole moments and then perform a Fourier transform. Figure 6 shows the power spectra of the dipole acceleration $|\ddot{d}_i(\omega)|^2(i=x,y)$ in the unit of Å^2 fs^{-2} as a function of energy. We refer to the power spectra of the dipole acceleration as harmonic-generation (HG) spectra. The HG spectra in Figs. 6(a)–6(d) correspond to the induced dipole moments in Figs. 4(a)–4(d), respectively. The red and the dashed black curves represent $|\ddot{d}_x(\omega)|^2$ and $|\ddot{d}_y(\omega)|^2$. Comparing Figs. 6(a) and 6(b), the harmonics along the x axis ($\ddot{d}_x$) seem relatively easier to generate than that along the y axis ($\ddot{d}_y$). A comparatively large peak appears at around 6 eV in Fig. 6(a). As discussed in the time evolution of the electron density in Fig. 3, this large peak is due to the fact that the sixth harmonics is accidentally close to a dipole resonance peak (=5.75 eV) of NC_6N. Despite the inversion symmetry of NC_6N, the nonuniform electric field, in contrast to the uniform one, causes the even harmonics in addition to the odd harmonics as shown in Figs. 6(c) and 6(d). Interestingly, the even and odd harmonics are, respectively, due to the induced dipole moments along the x and y axes. The even harmonics, therefore, have proved to be generated by the nonuniform electric field breaking the symmetry along the x axis. Furthermore, in comparison with the HG spectra by the uniform electric field, relatively higher harmonics are clearly seen in the HG spectra by the nonuniform electric field. In addition, their peak intensities do not decay linearly against the order of the harmonics. The investigation on the physics behind this nonlinear behavior is underway.

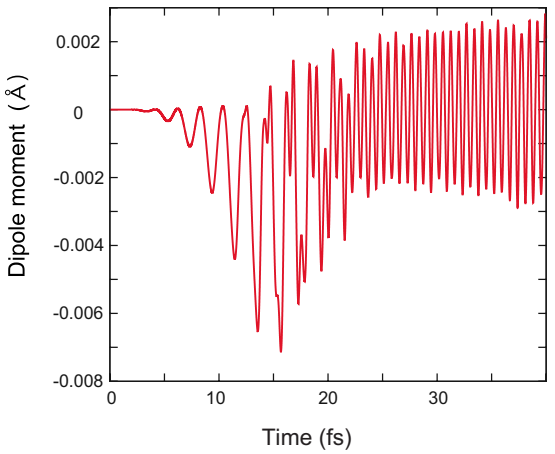

FIG. 5. (Color online) Magnification of d_x in Fig. 4(d).

Before ending this section, we demonstrate that the nonuniform electronic excitation also induces the quadrupole moment, which is never induced by the uniform electric field, as one of the phenomena beyond the dipole approximation. Such nondipole excitation was observed in an experiment [47], and suggested in a theoretical study [18], although both nanostructure systems are different from the present one. The xy component of the quadrupole moment (Q_{xy}) for the time evolution of Fig. 3(d) and its HG power spectrum are shown in Figs. 7(a) and 7(b), respectively. The

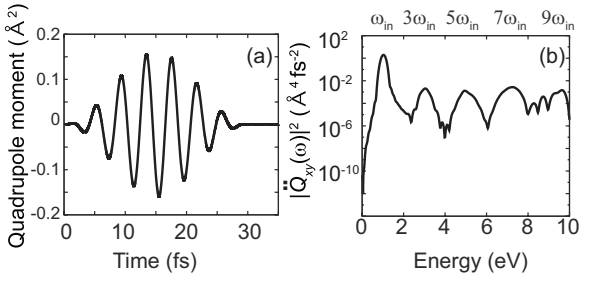

FIG. 7. (a) xy component of the induced quadrupole moment as a result of the nonuniform excitation with $\mu=5$ D and (b) its power spectrum.

TABLE I. Matrix elements of the second-order dipole moments along the x and y axes in the power of V_{eff}. e and o denote even and odd symmetries, respectively. The symmetries of the ground state and V_{eff} are indicated by bold characters.

$d_x^{(2)}$		$\langle 0\|x\|i\rangle$	$\langle i\|V_{\mathrm{eff}}\|j\rangle$	$\langle j\|V_{\mathrm{eff}}\|0\rangle$	
	$\int dx$	$\langle \boldsymbol{e}\|\boldsymbol{o}\|o\rangle$	$\langle o\|\boldsymbol{eo}\|eo\rangle$	$\langle eo\|\boldsymbol{eo}\|\boldsymbol{e}\rangle$	$\neq 0$
	$\int dy$	$\langle \boldsymbol{e}\|\|e\rangle$	$\langle e\|\boldsymbol{o}\|o\rangle$	$\langle o\|\boldsymbol{o}\|\boldsymbol{e}\rangle$	$\neq 0$
	$\int dz$	$\langle \boldsymbol{e}\|\|e\rangle$	$\langle e\|\boldsymbol{e}\|e\rangle$	$\langle e\|\boldsymbol{e}\|\boldsymbol{e}\rangle$	$\neq 0$
$d_y^{(2)}$		$\langle 0\|y\|i\rangle$	$\langle i\|V_{\mathrm{eff}}\|j\rangle$	$\langle j\|V_{\mathrm{eff}}\|0\rangle$	
	$\int dx$	$\langle \boldsymbol{e}\|\|e\rangle$	$\langle e\|\boldsymbol{eo}\|eo\rangle$	$\langle eo\|\boldsymbol{eo}\|\boldsymbol{e}\rangle$	$\neq 0$
	$\int dy$	$\langle \boldsymbol{e}\|\boldsymbol{o}\|o\rangle$	$\langle o\|\boldsymbol{o}\|e\rangle$	$\langle e\|\boldsymbol{o}\|\boldsymbol{e}\rangle$	$=0$
	$\int dz$	$\langle \boldsymbol{e}\|\|e\rangle$	$\langle e\|\boldsymbol{e}\|e\rangle$	$\langle e\|\boldsymbol{e}\|\boldsymbol{e}\rangle$	$\neq 0$

quadrupole moments both in the time and the energy domains provide the structural patterns quite similar to those of the dipole ones. To verify that Q_{xy} is non-negligible in the nonuniform excitation, we consider the charge distribution that causes dipole and quadrupole moments. The calculated value of the quadrupole moment in the unit of Å^2 is about an order of magnitude larger than that of the dipole moment in the unit of Å. The dipole moment of two charges q and $-q$ with the inter charge distance a is qa Å, whereas the quadrupole moment of two positive q' and two negative $-q'$ charges disposed at the corners of a square with its side being a is $q'a^2$ Å^2. Then, $|Q_{xy}| \sim 10|d_y|$ [see Figs. 4(d) and 7(a)] and a is ~ 10 Å for NC_6N. Thus, we have $q \sim q'$ because $q'a^2 \sim 10 \times qa \rightarrow q'a \sim 10 \times q \rightarrow q' \sim q$. This indicates that the dipolelike and quadrupolelike charge distributions have been induced in almost the same amount as a consequence of the nonuniform light-matter interaction.

B. Even and odd harmonics

Let us next carry out a perturbation analysis of the HG power spectra generated through the nonuniform light-matter interaction. As shown in Figs. 6(c) and 6(d), the even harmonics appear despite the inversion symmetry of NC_6N. The even and odd harmonics are due to the induced dipole moments d_x and d_y, respectively. This even and odd alteration is easily understood in terms of the symmetries of the molecular wave functions and the external field.

According to the time-dependent perturbation theory [48,49], nth dipole moment $d_\alpha^{(n)}$ ($n=1,2,\ldots$ and $\alpha=x,y,z$) in powers of the perturbation V_{eff} can be evaluated by the following matrix elements,

$$\langle 0|\alpha|i\rangle \underbrace{\langle i|V_{\mathrm{eff}}|j\rangle\langle j|V_{\mathrm{eff}}|k\rangle \cdots \langle l|V_{\mathrm{eff}}|0\rangle}_{n \text{ brackets}}, \tag{21}$$

where $|0\rangle$ and $|i\rangle$ are the ground and the excited eigenstates of the nonperturbative Hamiltonian of the molecule, respectively. As typical examples, $d_x^{(2)}$, $d_y^{(2)}$, $d_x^{(3)}$, and $d_y^{(3)}$ are considered. Table I summarizes the evaluation of the matrix elements of $d_x^{(2)}$ and $d_y^{(2)}$. The symmetries of the eigen states and the applied field are labeled as "e" for the even symmetry and "o" for the odd one. Since NC_6N has mirror symmetries in every direction, the eigenstate $\{|i\rangle\}$ is either even or odd with respect to x, y, or z axis, namely, $\psi(x,y,z) = \pm\psi(-x,y,z)$, $\psi(x,y,z) = \pm\psi(x,-y,z)$, or $\psi(x,y,z) = \pm\psi(x,y,-z)$. The effective potential V_{eff} given by Eq. (15) is neither an even nor an odd function of x, an odd function of y, and an even function of z, i.e., $V_{\mathrm{eff}}(x,y,z) \neq V_{\mathrm{eff}}(-x,y,z)$, $V_{\mathrm{eff}}(x,y,z) = -V_{\mathrm{eff}}(x,-y,z)$, and $V_{\mathrm{eff}}(x,y,z) = V_{\mathrm{eff}}(x,y,-z)$. Thus, the brackets can be estimated by decomposing them into the integrations with respect to the x, y, and z coordinates. $\int d\alpha(\alpha=x,y,z)$ in Table I denotes each component of the integrations. The symmetries of the ground state $|0\rangle$, the operators (x and y), and the potential V_{eff} are specified in bold characters. The symmetries of $|i\rangle$ and $|j\rangle$ are then specified so that the matrix elements have nonzero values. As a result, $d_x^{(2)}$ becomes nonzero, but $d_y^{(2)}$ must be zero because the integral of $\langle j|V_{\mathrm{eff}}|0\rangle$ with respect to the y coordinate vanishes. The same analysis can be applied to $d_\alpha^{(3)}$ (see, Table II). Then, $d_x^{(3)}$ must be zero but $d_y^{(3)}$ becomes nonzero. The above analysis clearly explains the even-odd alteration appears in the HG power spectra obtained by the nonuniform excitation.

C. Control of harmonic generation

Finally, it is demonstrated that the harmonics induced by the near field can be controlled. Figure 8 shows the HG power spectra obtained when both ends of the NC_6N mol-

TABLE II. Same as Table I but for the third-order dipole moments. As in the case of Table I, $\int dxdz$ is always nonzero, and thus only $\int dy$ is summarized here.

$d_x^{(3)}$		$\langle 0\|x\|i\rangle$	$\langle i\|V_{\mathrm{eff}}\|j\rangle$	$\langle j\|V_{\mathrm{eff}}\|k\rangle$	$\langle k\|V_{\mathrm{eff}}\|0\rangle$	
	$\int dy$	$\langle \boldsymbol{e}\|\|e\rangle$	$\langle e\|\boldsymbol{o}\|o\rangle$	$\langle o\|\boldsymbol{o}\|e\rangle$	$\langle e\|\boldsymbol{o}\|\boldsymbol{e}\rangle$	$=0$
$d_y^{(3)}$		$\langle 0\|y\|i\rangle$	$\langle i\|V_{\mathrm{eff}}\|j\rangle$	$\langle j\|V_{\mathrm{eff}}\|k\rangle$	$\langle k\|V_{\mathrm{eff}}\|0\rangle$	
	$\int dy$	$\langle \boldsymbol{e}\|\boldsymbol{o}\|o\rangle$	$\langle o\|\boldsymbol{o}\|e\rangle$	$\langle e\|\boldsymbol{o}\|e\rangle$	$\langle o\|\boldsymbol{o}\|\boldsymbol{e}\rangle$	$\neq 0$

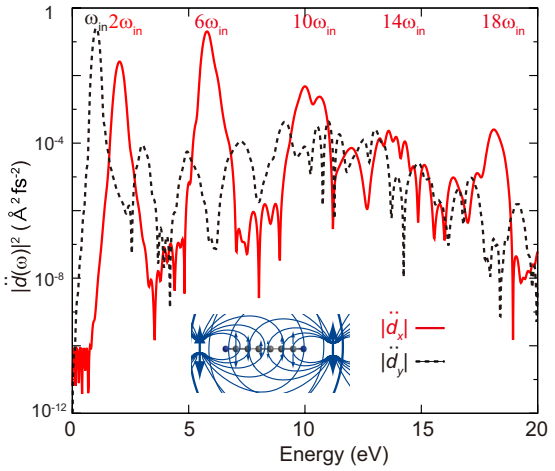

FIG. 8. (Color online) Power spectra of the dipole acceleration along the x and y axes. Two oscillating dipole fields with different phases disposed at both ends of the molecule are applied.

ecule are excited by the near fields radiated from two oscillating dipoles with different phases by $\pi/2$. The inset illustrates the schematic of the near-field excitation by two radiation sources. It is clearly seen from the figure that harmonics selectively appear every $4\omega_{\mathrm{in}}$ starting from the second harmonics ($2\omega_{\mathrm{in}}$). The forth and eighth harmonics ($4\omega_{\mathrm{in}}$ and $8\omega_{\mathrm{in}}$) completely disappear as a result of the interference between the two near-fields having different phases. We expect that this idea of the near-field excitation with different phases can control intensities and orders of HG spectra.

V. CONCLUDING REMARKS

We have presented a generalized theoretical description of optical response in an effort to understand a nonuniform light-matter interaction between a near field and a 1-nm-sized molecule. The light-matter interaction based on the multipolar Hamiltonian was described in terms of a space integral of the inner product of the total polarization of a molecule and an external electric field. Noteworthy is the fact that the polarization in the integral can be treated entirely without invoking any approximation such as a dipole approximation. Therefore, the present light-matter interaction theory allows us to understand the inhomogeneous electron dynamics associated with local electronic structures of a molecule at the 1 nm scale, although the wavelength of an incident laser pulse is much longer than the size of the molecule. For a computational application, we have studied the near-field-induced electron dynamics of NC_6N by using the TD-KS approach incorporated with the present nonuniform interaction theory. The electron dynamics induced by the nonuniform light-matter interaction is completely different from that by the conventional uniform interaction under the dipole approximation. Specifically, in the nonuniform electronic excitation high harmonics were generated more easily and much more interestingly the even harmonics were also generated in addition to the odd ones despite the inversion symmetry of NC_6N. Perturbation theory clearly explained that the even harmonics were generated owing to the symmetry-breaking (nonuniform) electric field along the x axis radiated from the oscillating dipole. It has also been found that the nonuniform fields with different phases control HG though their interference effect. We expect that the nonuniform electronic excitation can induce unprecedented electron dynamics giving information about local electronic structures, electronic transitions beyond the dipole approximation, and high-order nonlinear optical phenomena. Furthermore, the present nonuniform light-matter interaction/TD-KS approach incorporated with the Maxwell equations will enable us to elucidate electron and electromagnetic field dynamics in nanostructures.

ACKNOWLEDGMENTS

The present work was supported by Grant-in-Aid (Grants No. 18066019 and No. 21350018) and by the Next-Generation Supercomputer Project from the Ministry of Education, Culture, Sports, Science and Technology of Japan. T.I. acknowledges financial support by Japan Society for the Promotion of Science (Grant No. 2003281).

[1] S. A. Maier, P. G. Kik, H. A. Atwater, S. Meltzer, E. Harel, B. E. Koel, and A. A. G. Requicha, Nature Mater. **2**, 229 (2003).
[2] P. N. Prasad, *Nanophotonics* (Wiley-Interscience, Hoboken, NJ, 2004).
[3] C. Girard, Rep. Prog. Phys. **68**, 1883 (2005).
[4] L. Novotny and B. Hecht, *Principles of Nano-Optics* (Cambridge University Press, Cambridge, England, 2006).
[5] S. A. Maier, *Plasmonics: Fundamentals And Applications* (Springer-Verlag, Berlin, 2007).
[6] M. Moskovits, Rev. Mod. Phys. **57**, 783 (1985).
[7] K. Imura, H. Okamoto, M. K. Hossain, and M. Kitajima, Nano Lett. **6**, 2173 (2006).
[8] D. W. Brandl, N. A. Mirin, and P. Nordlander, J. Phys. Chem. B **110**, 12302 (2006).
[9] J. Zhao, A. O. Pinchuk, J. M. Mcmahon, S. Li, L. K. Ausman, A. L. Atkinson, and G. C. Schatz, Acc. Chem. Res. **41**, 1710 (2008) and references therein.
[10] K. Cho, Prog. Theor. Phys. Suppl. **106**, 225 (1991).
[11] J. K. Jenkins and S. Mukamel, J. Chem. Phys. **98**, 7046 (1993).
[12] O. Keller, Phys. Rep. **268**, 85 (1996).
[13] H. Ishihara, J. Phys.: Condens. Matter **16**, R247 (2004).
[14] D. Abramavicius and S. Mukamel, J. Chem. Phys. **124**, 034113 (2006).
[15] K. Lopata, D. Neuhauser, and R. Baer, J. Chem. Phys. **127**, 154714 (2007).
[16] J. Y. Yan, W. Zhang, S. Q. Duan, X. G. Zhao, and A. O. Govorov, Phys. Rev. B **77**, 165301 (2008).
[17] K. Lopata and D. Neuhauser, J. Chem. Phys. **130**, 104707 (2009).

[18] T. Iida and H. Ishihara, Phys. Status Solidi A **206**, 980 (2009).
[19] E. Lorin, S. Chelkowski, and A. Bandrauk, Comput. Phys. Commun. **177**, 908 (2007).
[20] C. Cohen-Tannoudji, J. Dupont-Roc, and G. Grynberg, *Photons and Atoms - Introduction to Quantum Electrodynamics* (Wiley-Interscience, New York, 1989).
[21] D. P. Craig and T. Thirunamachandran, *Molecular Quantum Electrodynamics* (Dover Publications, New York, 1998).
[22] S. Mukamel, *Principles of Nonlinear Optical Spectroscopy, Oxford Series on Optical and Imaging Sciences* (Oxford University Press, New York, 1999).
[23] K. Yabana and G. F. Bertsch, Phys. Rev. B **54**, 4484 (1996).
[24] K. Nobusada and K. Yabana, Phys. Rev. A **70**, 043411 (2004).
[25] K. Shiratori, K. Nobusada, and K. Yabana, Chem. Phys. Lett. **404**, 365 (2005).
[26] K. Nobusada and K. Yabana, Phys. Rev. A **75**, 032518 (2007).
[27] J. D. Jackson, *Classical Electrodynamics*, 3rd ed. (Wiley, New York, 1998).
[28] E. Runge and E. K. U. Gross, Phys. Rev. Lett. **52**, 997 (1984).
[29] F. Calvayrac, P. G. Reinhard, E. Suraud, and C. A. Ullrich, Phys. Rep. **337**, 493 (2000).
[30] M. A. L. Marques, A. Castro, G. F. Bertsch, and A. Rubio, Comput. Phys. Commun. **151**, 60 (2003).
[31] N. Troullier and J. L. Martins, Phys. Rev. B **43**, 1993 (1991).
[32] L. Kleinman and D. M. Bylander, Phys. Rev. Lett. **48**, 1425 (1982).
[33] J. P. Perdew and A. Zunger, Phys. Rev. B **23**, 5048 (1981).
[34] I. Vasiliev, S. Ogut, and J. R. Chelikowsky, Phys. Rev. B **65**, 115416 (2002).
[35] A. Wasserman, N. T. Maitra, and K. Burke, Phys. Rev. Lett. **91**, 263001 (2003).
[36] G. F. Gabriele and G. Vignale, *Quantum Theory of the Electron Liquid* (Cambridge University Press, Cambridge, England, 2005).
[37] F. Cataldo, Polyhedron **23**, 1889 (2004).
[38] TURBOMOLE VERSION 5.10 (2008), Quantum Chemistry Group, University of Karlsruhe: Karlsruhe, Germany.
[39] R. Ahlrichs, M. Bär, M. Häser, H. Horn, and C. Kölmel, Chem. Phys. Lett. **162**, 165 (1989).
[40] J. P. Perdew and Y. Wang, Phys. Rev. B **45**, 13244 (1992).
[41] A. Schäfer, H. Horn, and R. Ahlrichs, J. Chem. Phys. **97**, 2571 (1992).
[42] These bond lengths remain almost unchanged (i.e., at most 0.0024 Å for C_3-C_4) even if the geometry optimization was performed by using the B3LYP functional [50,51].
[43] K. Yabana and G. F. Bertsch, Int. J. Quantum Chem. **75**, 55 (1999).
[44] J. R. Chelikowsky, N. Troullier, K. Wu, and Y. Saad, Phys. Rev. B **50**, 11355 (1994).
[45] K. Burnett, V. C. Reed, J. Cooper, and P. L. Knight, Phys. Rev. A **45**, 3347 (1992).
[46] T. Brabec and F. Krausz, Rev. Mod. Phys. **72**, 545 (2000).
[47] S. Tojo and M. Hasuo, Phys. Rev. A **71**, 012508 (2005).
[48] J. J. Sakurai, *Modern Quantum Mechanics* (Revised Edition) (Addison Wesley, Reading, 1993).
[49] R. W. Boyd, *Nonlinear Optics*, 3rd ed. (Academic Press, New York, 2008).
[50] C. T. Lee, W. T. Yang, and R. G. Parr, Phys. Rev. B **37**, 785 (1988).
[51] A. D. Becke, J. Chem. Phys. **98**, 5648 (1993).